BMC Cancer

RESEARCH

Open Access

Assessing the causal association between 731 immunophenotypes and the risk of colorectal cancer: a Mendelian randomization study

Fei Gao[1†], Qiaoli Zhang[1†], Fei Teng[1†], Liling Li[1], Honglin Jiang[1], Wenna Li[1], Chenxi Hu[1], Zhongwen Lu[1], Yuxiang Wan[1*] and Jinchang Huang[1*]

Abstract

Background Emerging research suggested a potential role of immune cells in colorectal cancer (CRC) development. However, the causal relationship between immune phenotypes and CRC remains elusive. Hence, this two-sample Mendelian randomization (MR) study aimed to explore the causal association.

Methods In this study, a bidirectional, two-sample MR analysis and multivariate MR was conducted, leveraging public genetic data. Four types of immune phenotypes were employed. A comprehensive sensitivity analysis was carried out to validate the robustness, heterogeneity, and horizontal pleiotropy of the results, with Bonferroni correction applied for accurate interpretation.

Results It was revealed that four immune cell phenotypes were significantly associated with CRC risk. Specifically, lymphocyte % leukocyte in the T-cell/B-cell/NK-cell (TBNK) group (odds ratio (OR) = 1.0013, 95% confidence interval (CI): 1.0005–1.0017, $P = 0.0003$, $P_{Bonferroni} = 0.011$) and CD3 on CM CD8br in the maturation stages of T cell group (OR = 1.0014, 95% CI: 1.0006–1.0022, $P = 0.0007$, $P_{Bonferroni} = 0.023$) were positively correlated with the risk of CRC. Conversely, DN ($CD4^{-}CD8^{-}$) %leukocyte in the TBNK group (OR = 0.9990, 95% CI: 0.9984–0.9997, $P = 0.0020$, $P_{Bonferroni} = 0.063$) and herpesvirus entry mediator (HVEM) on CD8br in the maturation stages of T cell group (OR = 0.9989, 95% CI: 0.9982–0.9997, $P = 0.00431$, $P_{Bonferroni} = 0.137$) exhibited a negative association with the risk of CRC. This study did not detect any statistically significant impact of CRC on immune phenotypes.

Conclusions This study inferred an association between immune cells and CRC risk. Nevertheless, further clinical and experimental studies are warranted to validate these findings and elucidate the underlying mechanisms.

Keywords Immunocyte, Immunocyte phenotype, Mendelian randomization, Colorectal cancer

Introduction

Colorectal cancer (CRC) ranks as the third most common malignancy globally, with the third and second highest incidences and mortality rates among all malignancies, respectively. The mortality rate is alarming, with CRC claiming over 900,000 lives annually [1]. Overall, the incidence of CRC is rising globally, particularly in low- and middle-income countries. Conversely, in high-income

†Fei Gao, Qiaoli Zhang and Fei Teng contributed equally to this work.

*Correspondence:
Yuxiang Wan
wanyuxiang@bucm.edu.cn
Jinchang Huang
zryhhuang@163.com
[1] The Third Affiliated Hospital, Beijing University of Chinese Medicine, Beijing 100029, China

countries, particularly those with established screening programs, the incidence of CRC is stabilizing or declining [2].

The pathogenesis of CRC is primarily attributed to a range of modifiable risk factors, including smoking, alcohol consumption, obesity, lack of physical activity, unhealthy dietary habits, and inflammatory bowel disease (IBD) [2, 3]. Additionally, genetic factors, such as familial adenomatous polyposis (FAP) are significantly associated with the development of CRC [4]. Despite recent advances in CRC detection and treatment, CRC remains a major challenge in clinical practice, and the role of the immune system in combating CRC has noticeably attracted oncologists' attention.

Immune cells constitute a critical component of the tumor microenvironment (TME) and play a pivotal role in the treatment of diverse types of cancer [5]. These cells recognize and eliminate malignant cells to exert immune surveillance functions. However, in certain circumstances, tumor cells can evade immune surveillance. Immune cells contribute to the likelihood of cancer development and support all stages of tumorigenesis. Cancer cells are involved in coordinated interaction of neighboring stromal cells with inflammatory cells, leading to the creation of an inflammatory TME. CRC is a complex and heterogeneous disease characterized by dysregulation of the interaction between tumor cells and the immune system. The TME plays a crucial role in the onset and progression of cancer. Myeloid immune cells, such as dendritic cells and macrophage subsets, exert diverse roles in cancer immunity, in which they exert antitumor effects, while they may also contribute to tumor growth [6]. Tumor-associated macrophages, as abundant and actively infiltrating inflammatory cells in the TME, play a notable function in CRC [7]. It is noteworthy that research in this field is dynamic, and ongoing studies continue to enhance our understanding of the immune landscape of CRC. Therefore, it is essential to always refer to the latest literature for updated information. Given the current challenges, it is estimated that 50% of CRC cases are preventable [8]. Consequently, there is a need to prioritize the identification of novel risk factors to develop subsequent prevention and treatment strategies, thereby alleviating the future healthcare burden.

In epidemiological research, Mendelian randomization (MR) serves as an analytical tool to assess etiological inferences and explore the relationship between risk factors (exposures) and outcomes. Advancements in genetic research could further promote investigating the causal relationship between 731 immune cell phenotypes and the risk of CRC. In the present study, genetic variations as instrumental variables (IVs) were assessed using MR analysis [9], examining the bidirectional causal relationship between immune cells and the risk of CRC risk. This approach provides a novel perspective for understanding the genetic correlation between immune cells and the risk of CRC.

Materials and methods

Study design

A bidirectional two-sample MR analysis and multivariate MR was conducted to assess the causal relationship between 731 immune cell phenotypes (grouped into seven categories) and the risk of CRC.

Firstly, GWAS data of 731 immune cell phenotypes (GCST90001391 to GCST90002121) were extracted from the GWAS Catalog [10]. Secondly, GWAS data of CRC were obtained based on summary statistics from Europeans. Utilizing large-scale GWAS summary datasets, a bidirectional two-sample MR analysis was performed. Five methods were employed for causal inference, including MR-Egger, weighted median, simple mode, and weighted mode. These methods could promote assessing the causal relationship between the 731 immune cell phenotypes and the risk of CRC. Subsequently, a reverse MR study was undertaken. Finally, the causal relationships between exposures and outcomes inferred through two-sample Mendelian randomization analysis will be further explored using MVMR to examine the potential causal relationships between multiple immune cell types and colorectal cancer.

This MR analysis was conducted using previously published and publicly available large-scale summary datasets. All participants provided written informed consent in the corresponding original GWAS studies. The study workflow is illustrated in Fig. 1.

Data sources

The GWAS summary statistics of 731 immune phenotypes are publicly available from the GWAS Catalog (GCST90001391 to GCST90002121) [10]. Additional file 1 provides detailed information for these 731 immunocyte phenotypes. Utilizing data from 3757 European individuals, the present study examined approximately 220,000 single-nucleotide polymorphisms (SNPs) after adjusting for sex and age. The analysis identified 122 significant independent association signals across 70 loci, revealing 53 novel loci [10].

To avoid population stratification, the GWAS summary statistics of CRC were downloaded from a large-scale GWAS conducted on individuals of European ancestry (Ncase=372,016, Ncontrol=5,657) with GWAS ID

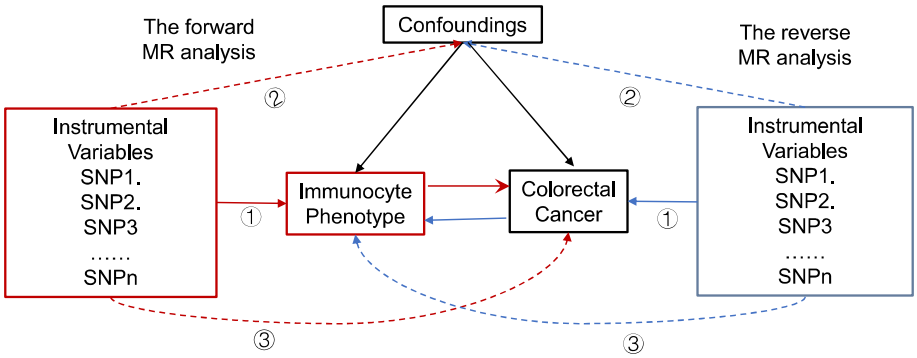

Fig. 1 Illustration of the three key assumptions underlying Mendelian randomization analysis. (1) Relevance Hypothesis: The instrumental variables (IVs) must exhibit a strong association with the exposure factors. (2) Independence Hypothesis: The IVs must remain unaffected by both known and unknown confounders. (3) Exclusion Hypothesis: The IVs can only influence outcome factors indirectly through the mediation of exposure factors

ieu-b-4965. This GWAS dataset, originating from the UK BioBank, comprised 5,657 CRC patients and 372,016 healthy controls. After undergoing quality control and imputation, approximately 11,738,639 SNPs were analyzed.

Screening of IVs

The selection of IVs in this study should adhere to three fundamental assumptions: (1) a direct association between the IVs and the exposure; (2) the absence of any association between IVs and potential confounding factors that might affect both the exposure and the outcome; and (3) IVs exerting no influence on the outcome through any pathway other than the exposure [11].

It was attempted to set the significance threshold for IVs of each immune phenotype at 1×10^{-5} [10]. This threshold is less strict than the commonly used 5×10^{-8}, but as previous studies have shown, smaller sample sizes in immune phenotypes do not require such stringent *p*-value correction thresholds [12–15]. And linkage disequilibrium analysis was undertaken in the range of 10,000 with $r^2<0.001$. For CRC, the significance threshold was adjusted to 5×10^{-8}, and linkage disequilibrium analysis was conducted in the range of 10,000 with $r^2<0.001$. To eliminate the bias from weak IVs, the *F*-values for each IV were calculated using the formula from prior research: $F=R^2\times(N-2)/(1-R^2)$; $R^2=2\times EAF\times(1-EAF)\times\beta^2$ [16]. IVs with $F>10$were subsequently included in the MR analysis [16]. To identify and exclude confounders related to CRC outcomes, Phenoscanner (http://www.phenoscanner.medschl.cam.ac.uk/) was utilized in conjunction with Ldlink (https://ldlink.nih.gov/?tab=ldtrait) [17]. SNPs associated with confounders, such as IBD, red meat consumption, waist-to-hip ratio, body mass index, obesity, alcohol drinking, smoking, and others [18–20] were excluded from the analysis. The list of excluded SNPS associated with confounding factors is uploaded in Additional file 2. The remaining IVs were retained for further analysis.

Data analysis

Data analysis was conducted using R 4.3.2 software (http://www.R-project.org). MR analysis was performed using the TwoSampleMR package (version 0.5.10), while the MRPRESSO package (version 1.0) was utilized to identify outliers and detect pleiotropy through the application of MRPRESSO analysis. After obtaining confounders through Phenoscanner and Ldlink, SNPs associated with these confounders were excluded using R programming language.

For the causal analysis between exposure and outcome, the IVW method, as the primary analytical approach, was employed to investigate the causal relationship between 731 immune phenotypes and the risk of CRC. Complementary analyses were conducted using the weighted median, simple mode, weighted mode, and MR-Egger regression tests. The IVW method assumes that all SNPs included in the analysis serve as valid IVs and provides the most accurate estimation in the absence of horizontal pleiotropy [21].

To exclude the influence of horizontal pleiotropy, the MR-Egger regression test was applied to assess gene pleiotropy. The intercept being close to zero indicates the absence of significant heterogeneity [22]. MR-PRESSO method was utilized to detect the presence of outliers and correct for gene pleiotropy. The leave-one-out analysis was employed to exclude each SNP and assess the impact of the remaining IVs on the results, aiming to identify any individual SNP that could significantly affect the outcome [23]. The effect sizes in this study were expressed as odds ratios (OR) with 95% confidence intervals (CI). Additionally, scatter plots and funnel plots were drawn. The scatter plots demonstrated that the results were not influenced

by outliers, while the funnel plots showed the robustness of the associations and the absence of heterogeneity. To explore reverse causality, a reverse MR analysis was conducted using the same methods for immune cell phenotypes and the risk of CRC, and the range of MR estimates was represented by β values. The statistical power of the MR analysis was calculated using the available web tool (https://shiny.cnsgenomics.com/mRnd/), with a power greater than 80% considered an excellent value [24]. Furthermore, to account for the challenge of multiple testing, Bonferroni correction was employed on the *P*-values using the Bioladder online tool (https://www.bioladder.cn/web/#/pro/index). According to previous studies, $P_{Bonferroni}$ value less than 0.2 was indicative of a causal relationship, while a $P_{Bonferroni}$ value less than 0.05 indicated a significant causal relationship [25].

Multivariate MR analysis

MVMR effectively captures the interactions between genetic variations associated with various exposures that may potentially influence each other [26]. Given the significant statistical relationships between immune cell phenotypes, we conducted a series of MVMR analyses in this study to elucidate the distinct causal relationships between multiple immune cell phenotypes and colorectal cancer risk. Our MVMR analysis employed the IVW strategy, a meticulous approach that enhances precision and strengthens the integrity of causal inferences [27].

Cross-trait linkage disequilibrium score regression analysis

To assess whether immune phenotypes share a polygenic architecture with colorectal cancer, we conducted a cross-trait linkage disequilibrium score regression (LDSC) analysis. This analysis was performed to calculate the genetic correlation, which can be biased when two GWAS studies involve overlapping individuals [28]. LDSC provides a more accurate and unbiased estimate of genetic correlation. We used the LDSC package in R software (version 4.3.1) for these calculations, as described on GitHub.

Results

Positive IVs

In this study, IVs obtained from GWAS data of 731 immune cell phenotypes were screened. All selected IVs exhibited F-statistics greater than 10, ensuring the absence of weak IV bias. The *F*-value list is provided in Additional file 3. Table 1 lists SNPs screened for all positive results.

The causal relationship between immunophenotypes and the risk of CRC

A total of 32 immune phenotypes were identified that exhibited causal relationship with the risk of CRC. Specifically, 12 immune phenotypes were associated with a decreased risk of CRC, while 20 immune phenotypes were linked to an increased risk of CRC. These 32 immune cell phenotypes spanned several cellular categories: B cells (7 phenotypes), regulatory T (Treg) cells (10 phenotypes), myeloid cells (2 phenotypes), T-cell/B-cell/NK-cell (TBNK) (5 phenotypes), Maturation stages of T cells (6 phenotypes), monocytes (1 phenotype), and conventional dendritic cell (cDC) (1 phenotype). Notably, the monocyte immune cell type showed a significant causal relationship only with a decreased risk of CRC, rather than with an increased risk. Conversely, the cDC immune cell type exhibited a significant causal link only with an increased risk of CRC, rather than with a decreased risk. The genetically predicted results from the IVW method for the immune cells and the risk of CRC are presented in Fig. 2.

Notably, 12 protective factors ($OR < 1$, $P < 0.05$) were identified, including 5 B cell phenotypes: naive-mature B cell AC; $CD24^+$ $CD27^+$ %B cell; transitional %lymphocyte; CD20 on IgD^+ $CD24^-$; and IgD on IgD^+ $CD38^-$. Additionally, two Treg phenotypes were found, including $CD39^+$ $CD4^+$ %T cell and CD25hi $CD45RA^-$ CD4 not Treg %T cell. Among myeloid cells, one protective factor was identified: Immature Myeloid-Derived Suppressor Cells %CD33dim HLA DR^- $CD66b^{-\cdot}$ Furthermore, 2 maturation stages of T cell phenotypes were found to be protective, involving herpesvirus entry mediator (HVEM) on EM CD8br and HVEM on CD8br. Additionally, CCR2 on monocyte represented a protective factor among monocytes. Lastly, DN ($CD4^-CD8^-$) %leukocyte was identified as a protective factor in the TBNK category.

Furthermore, 20 risk factors ($OR > 1$, $P > 0.05$) were identified as follows: 2 species of B cells, including BAFF-R on naive-mature B cell and BAFF-R on B cell; one species of cDC, specifically $CD62L^-$plasmacytoid DC AC; 4 species related to the maturation stages of T cells, such as CD3 on EM $CD4^+$, CD3 on CM CD8br, CD4 on $CD4^+$, and CD4 on $CD45RA^+$ $CD4^+$; one species of myeloid cells, CD33br HLA DR^+ $CD14^-$AC; 4 species in the TBNK group, including T cell %leukocyte, T cell %leukocyte, CD3 on HLA DR^+ CD8br, and FSC-A on B cell; and 8 species of Treg cells, such as resting Treg %CD4 Treg, resting Treg %CD4, $CD28^+$ $CD45RA^+$ CD8br AC, CD3 on $CD39^+$ $CD4^+$, CD3 on $CD28^+$ $CD45RA^+$ CD8br, CD3 on $CD28^-$ CD8br, CD25 on secreting Treg, and CD4 on $CD39^+$ activated Treg.

After applying the Bonferroni adjustment correction, 4 results retained statistical significance. Notably, lymphocyte %leukocyte in the TBNK group ($P_{Bonferroni} = 0.011$) and CD3 on CM CD8br in the maturation stages of T cell group ($P_{Bonferroni} = 0.023$) were identified as risk factors

Table 1 Number of SNPs selected in each step

ID	Trait	Number of SNPs after LD	Number of SNPs after F > 10	Number of final IVs
ebi-a-GCST90001470	CD62L- plasmacytoid DC AC	24	24	24
ebi-a-GCST90001481	Resting Treg % CD4 Treg	27	27	21
ebi-a-GCST90001482	Resting Treg %CD4	31	31	29
ebi-a-GCST90001518	CD33br HLA DR + CD14- AC	28	28	27
ebi-a-GCST90001602	Lymphocyte %leukocyte	22	22	21
ebi-a-GCST90001605	T cell %leukocyte	19	19	18
ebi-a-GCST90001690	CD28 + CD45RA + CD8br AC	54	54	48
ebi-a-GCST90001716	BAFF-R on naive-mature B cell	22	22	19
ebi-a-GCST90001829	BAFF-R on B cell	21	21	18
ebi-a-GCST90001843	CD3 on EM CD4 +	19	19	18
ebi-a-GCST90001846	CD3 on CM CD8br	18	18	17
ebi-a-GCST90001850	CD3 on HLA DR + CD8br	25	25	19
ebi-a-GCST90001860	CD3 on CD39 + CD4 +	28	28	23
ebi-a-GCST90001864	CD3 on CD28 + CD45RA + CD8br	24	24	20
ebi-a-GCST90001865	CD3 on CD28- CD8br	19	19	18
ebi-a-GCST90001941	CD25 on secreting Treg	14	14	13
ebi-a-GCST90001968	FSC-A on B cell	20	20	20
ebi-a-GCST90002022	CD4 on CD4 +	22	22	21
ebi-a-GCST90002027	CD4 on CD45RA + CD4 +	27	27	23
ebi-a-GCST90002067	CD4 on CD39 + activated Treg	22	22	21
ebi-a-GCST90001409	Naive-mature B cell AC	22	22	22
ebi-a-GCST90001417	CD24 + CD27 + %B cell	26	26	24
ebi-a-GCST90001512	CD25hi CD45RA- CD4 not Treg %T cell	31	31	30
ebi-a-GCST90001516	Im MDSC %CD33dim HLA DR- CD66b-	22	22	19
ebi-a-GCST90001578	Transitional %lymphocyte	27	27	23
ebi-a-GCST90001613	DN (CD4-CD8-) %leukocyte	18	18	18
ebi-a-GCST90001658	CD39 + CD4 + %T cell	31	31	27
ebi-a-GCST90001747	CD20 on IgD + CD24-	21	21	18
ebi-a-GCST90001822	IgD on IgD + CD38-	28	28	23
ebi-a-GCST90001873	HVEM on EM CD8br	18	18	13
ebi-a-GCST90001881	HVEM on CD8br	16	16	14
ebi-a-GCST90002008	CCR2 on monocyte	21	21	21

for CRC. Conversely, DN ($CD4^{-}CD8^{-}$) %leukocyte in the TBNK group ($P_{Bonferroni} = 0.063$) and HVEM on CD8br in the maturation stages of T cell group ($P_{Bonferroni} = 0.137$) were recognized as protective factors for CRC.

The results of 5 MR methods, are detailed in Additional file 4. Additionally, Additional file 5 provides scatter plots for 32 data items.

Forward sensitivity analysis

The sensitivity analysis revealed no heterogeneity in the causal relationship between the 32 immune cell phenotypes and the risk of CRC ($P > 0.05$ for Q-test). Additionally, there was no evidence of horizontal pleiotropy ($P > 0.05$ for MR-Egger's intercept method), supporting the reliability of the causal inference results (Table 2). Both the leave-one-out analysis and funnel plot indicated the robustness of the data (Additional file 5).MR-PRESSO results are provided in Additional file 6. The statistical power of all results is shown in Additional file 7.

Reverse IV results

In this study, we conducted a GWAS data-based IV selection for CRC, ensuring that all IVs had an *F*-value greater than 10 to eliminate any potential IV bias.

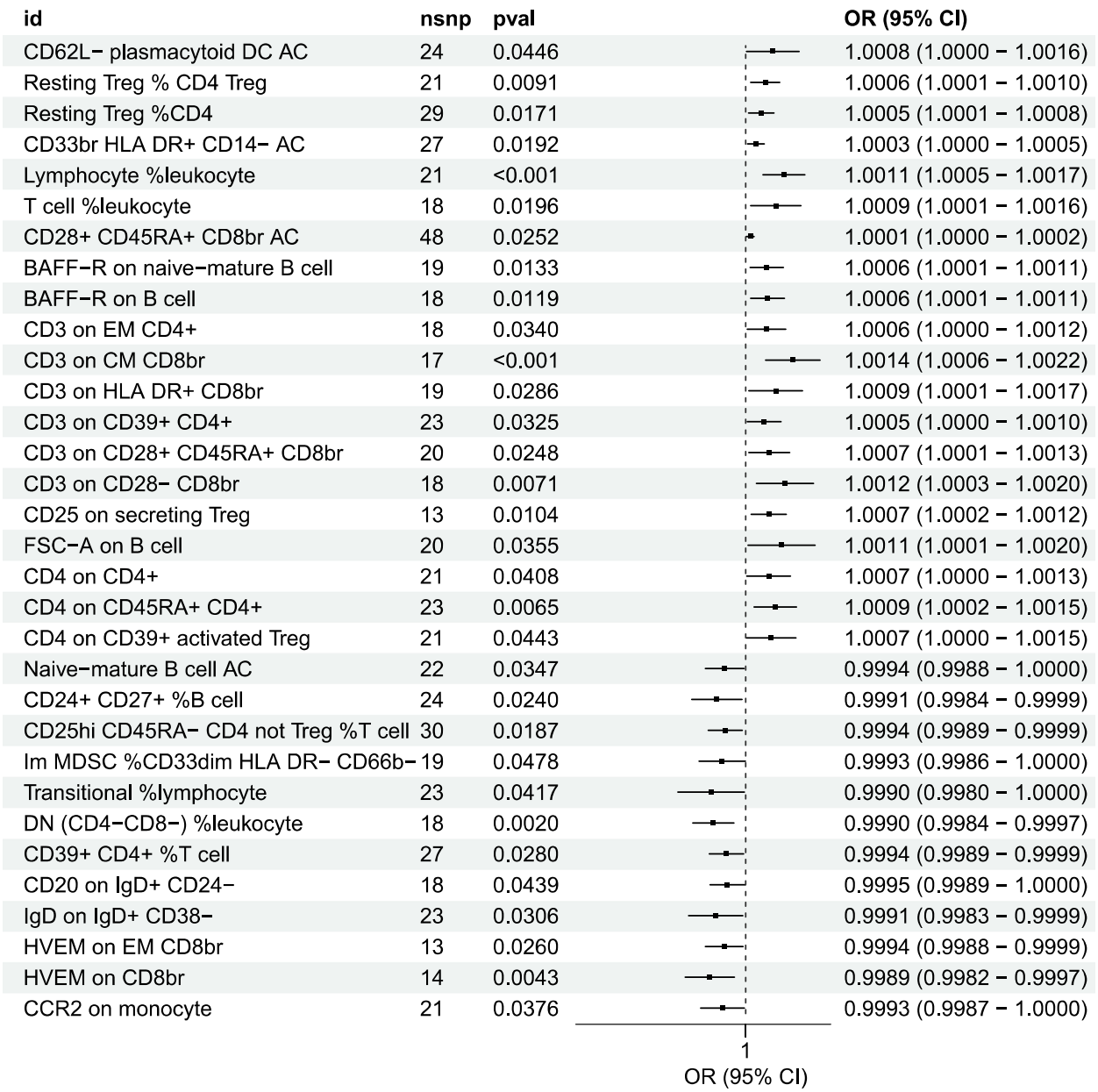

Fig. 2 Forward MR analysis utilizing the inverse variance weighting method

Table 3 presents the number of SNPs screened at each step of the selection process.

The causal relationship between the risk of CRC and immunophenotypes

A total of 36 immune phenotypes were identified, all exhibiting a causal relationship with the risk of CRC. These 36 immune phenotypes were categorized into 3 distinct groups: lymphocyte count (consisting of 3 phenotypes), leukocyte count (consisting of 1 phenotype), and blood protein measurement (consisting of 32 phenotypes). The genetically predicted results from the IVW method for the immune cells and the risk of CRC are presented in Fig. 3.

The lymphocyte count group included CD20- B cell %lymphocyte, $CD28^{-}$ $CD25^{++}$ $CD8^{+}$ T cell %CD8+T cell, and $CD25^{++}$ $CD8^{+}$ T cell %$CD8^{+}$ T cell. The leukocyte count group comprised $CD62L^{-}$ plasmacytoid Dendritic Cell Absolute Count. The blood protein measurement group encompassed BAFF-R on $CD24^{+}$ $CD27^{+}$ B cell, BAFF-R on IgD^{+} $CD24^{+}$ B cell, BAFF-R on IgD^{+} $CD24^{-}$ B cell, BAFF-R on IgD^{+} $CD38^{-}$ B cell, BAFF-R

Table 2 Positive MR sensitivity analysis

Panel	Immune traits	IVW		MR-Egger	
		Q	P	intercept	P
B cell	Naive-mature B cell AC	12.7404132	0.917443838	6.58E-05	0.565397462
B cell	CD24 + CD27 + %B cell	25.4489237	0.327561859	9.74E-05	0.572882785
cDC	CD62L- plasmacytoid DC AC	9.744737644	0.992747365	−1.72E-05	0.914540795
Treg	Resting Treg % CD4 Treg	25.269487	0.191315019	0.000145535	0.42912587
Treg	Resting Treg %CD4	26.41363903	0.550319227	6.07E-05	0.660309028
Treg	CD25hi CD45RA- CD4 not Treg %T cell	20.41342575	0.879612131	4.79E-06	0.970045006
Myeloid cell	Im MDSC %CD33dim HLA DR-CD66b-	26.10646486	0.097348418	1.31E-05	0.950608121
Myeloid cell	CD33br HLA DR + CD14- AC	22.36633755	0.668495855	−1.45E-05	0.897717076
B cell	Transitional %lymphocyte	19.86622761	0.591407259	9.91E-05	0.575235087
TBNK	Lymphocyte %leukocyte	21.64223734	0.360235024	7.47E-05	0.574565978
TBNK	T cell %leukocyte	21.3484692	0.211089836	1.35E-05	0.929340562
TBNK	DN (CD4-CD8-) %leukocyte	17.91663672	0.394118241	−5.44E-05	0.694317839
Treg	CD39 + CD4 + %T cell	20.8486648	0.749732881	1.09E-05	0.92366958
Treg	CD28 + CD45RA + CD8br AC	41.57944577	0.695898816	2.46E-05	0.779581422
B cell	BAFF-R on naive-mature B cell	17.45104872	0.492326868	6.39E-05	0.704730968
B cell	CD20 on IgD + CD24-	11.71419341	0.81712639	−9.72E-05	0.413539106
B cell	IgD on IgD + CD38-	32.86394042	0.063813546	−0.000262245	0.137100823
B cell	BAFF-R on B cell	17.18083653	0.442180928	6.55E-05	0.70578435
Maturation stages of T cell	CD3 on EM CD4 +	12.71713226	0.754906674	0.000270835	0.11213086
Maturation stages of T cell	CD3 on CM CD8br	13.9980488	0.598859203	0.000198965	0.314422349
TBNK	CD3 on HLA DR + CD8br	20.02132228	0.331620525	1.51E-05	0.943719224
Treg	CD3 on CD39 + CD4 +	7.663932595	0.997944116	−6.73E-05	0.671763276
Treg	CD3 on CD28 + CD45RA + CD8br	16.18034363	0.645213386	0.000218596	0.233138256
Treg	CD3 on CD28- CD8br	15.44209794	0.563670398	6.41E-05	0.759404213
Maturation stages of T cell	HVEM on EM CD8br	11.00267419	0.528689522	−0.000242004	0.246976203
Maturation stages of T cell	HVEM on CD8br	12.58989155	0.47996466	−0.000271331	0.224242141
Treg	CD25 on secreting Treg	9.485399981	0.661006344	−5.31E-05	0.74362229
TBNK	FSC-A on B cell	23.58868334	0.212405806	−8.94E-06	0.969593393
Monocyte	CCR2 on monocyte	25.73516546	0.174737783	−0.000109087	0.550190069
Maturation stages of T cell	CD4 on CD4 +	14.21935508	0.819202188	−0.00014371	0.384388944
Maturation stages of T cell	CD4 on CD45RA + CD4 +	11.35014126	0.969388494	−7.81E-05	0.678461769
Treg	CD4 on CD39 + activated Treg	29.97659576	0.070233782	0.000124428	0.540448094

on IgD^+ CD38dim B cell, BAFF-R on IgD^- $CD38^+$ B cell, BAFF-R on memory B cell, BAFF-R on naive-mature B cell, BAFF-R on unswitched memory B cell, BAFF-R on switched memory B cell, BAFF-R on IgD^+ B cell, CD20 on IgD^+ $CD38^-$ unswitched memory B cell, CD20 on IgD^- $CD38^+$ B cell,CD27 on Plasma Blast-Plasma Cell, CD38 on IgD^- CD38dim B cell, BAFF-R on B cell, CD3 on $CD39^+$ resting CD4 regulatory T cell, HVEM on Central Memory $CD8^+$ T cell, CD28 on $CD28^+$ $CD45RA^+$ $CD8^+$ T cell, CD28 on resting CD4 regulatory T cell, CD127 on T cell, CD127 on $CD28^+$ $CD45RA^+$ $CD8^+$ T cell, CD127 on $CD45RA^+$ $CD4^+$ T cell, CD33 on CD33dim HLA DR + $CD11b^+$, CD16 on $CD14^-$ $CD16^+$ monocyte, PDL-1 on $CD14^+$ $CD16^-$ monocyte, PDL-1 on $CD14^-$ $CD16^+$ monocyte, PDL-1 on $CD14^-$ $CD16^-$, PDL-1 on monocyte, CD39 on monocyte, CD11b on Granulocytic Myeloid-Derived Suppressor Cells, and HLA DR on $CD33^+$ HLA DR^+ $CD14^-$. The results of 5

Table 3 Number of SNPs screened at each step of the selection process

ID	Trait	Number of SNPs after LD	Number of SNPs after F > 10	Number of final IVs
ieu-b-4965	Colorectal cancer	8	8	8

MR methods are presented in Additional file 8. Additionally, Additional file 9 provides scatter plots for 36 data items.

However, after applying the Bonferroni adjustment correction, no statistically significant differences were found in the immune traits ($P_{Bonferroni} > 0.2$).

Reverse sensitivity analysis

The results of the reverse sensitivity analysis indicated that there was no heterogeneity in the causal relationship between the risk of CRC and the 36 immune cell phenotypes ($P > 0.05$ for Q-test). Additionally, there was no evidence of horizontal pleiotropy ($P > 0.05$ for MR-Egger's intercept method), supporting the reliability of the causal inference results (Table 4). Both the funnel plot and leave-one-out analysis confirmed the robustness of the data (Additional file 9).

This study also features a schematic summary figure (Fig. 4), depicting the results, aimed at enhancing understanding for readers unfamiliar with the subject.

MVMR analysis

To describe the potential causal relationships between selected immune cell phenotypes and colorectal cancer (CRC) incidence, we conducted MVMR analysis using statistically significant exposures derived from two-sample Mendelian randomization analysis, including Lymphocyte %leukocyte, CD3 on CM CD8br, DN (CD4-CD8-) %leukocyte, and HVEM on CD8br. CRC was used as the outcome. The analysis was performed using the IVW method. The IVW results indicated that Lymphocyte %leukocyte has a direct and independent causal relationship with CRC susceptibility (OR: 1.0056, 95% CI: 1.0007–1.0106, $P = 0.0261$). The results are shown in the Fig. 5 below.

Results of LDSC analysis

We conducted an analysis of the genetic correlation between HVEM on CD8 + T cells and colorectal cancer. The genetic correlation (Rg) was found to be 0.037, with a standard error of 0.212 and a *P*-value of 0.861. Consequently, there is no significant genetic correlation between HVEM on CD8 + T cells and colorectal cancer (Fig. 6).

However, during the LDSC analysis of lymphocyte %leukocytes, CD3 on CM CD8br, and DN (CD4-CD8-) % leukocytes, negative heritability was observed when examining the genetic correlation with colorectal cancer. This situation is not uncommon in genetic research and may be caused by various factors, such as random noise, population stratification, insufficient sample size, or poor sample quality.

Discussion

Utilizing vast quantities of publicly available genetic data, the causal relationship between 731 immune cell phenotypes and the risk of CRC was investigated. Additionally, we have tested the statistical validity of all MR analyses, although the results were somewhat limited. We hope it can offer valuable insights for future research. Through comprehensive genetic analysis, the present study provided evidence suggesting that immune cells may influence CRC risk. SNPs were employed as IVs in a bidirectional, two-sample MR analysis. The findings indicated that DN ($CD4^-CD8^-$) %leukocyte and HVEM on CD8bright T cells were associated with the reduced CRC incidence. Additionally, associations were found between lymphocyte %leukocyte and CD3 on central memory CD8bright T cells with an increased risk of CRC. The MVMR study further indicates that lymphocytes % leukocytes is associated with an increased risk of colorectal cancer. In the reverse Mendelian randomization analysis, no statistically significant causal relationship between CRC and immune phenotypes was observed. In this study, the results of LDSC are not satisfactory. The speculated reason may be that due to polygenic regulation, there are undiscovered confounding factors involved. However, it still enriches our research and offers new directions for future studies.

In the present study, a reduction was identified in the risk of CRC with increasing level of DN ($CD4^-CD8^-$) %leukocyte. DN T cells, classified as unconventional T cells, express the T lymphocyte antigen receptor, while lack the CD4, CD8, and CD56 surface markers is noteworthy. Prior studies have demonstrated the significant antitumor activity of DN T cells [29, 30]. Notably, Vγ9Vδ2 DN T cells have been identified as effective cytolytic mediators in cell-based immunotherapy against malignancies [31]. Furthermore, activated TCR-$\gamma\delta^+$ DN T cells secrete a high level of interferon-γ (IFN-γ), an essential cytokine in antitumor immune responses, suggesting their potential utilization in anticancer immunotherapy [32]. In vitro studies have demonstrated that human DN T cells, when cocultured with tumorigenic strains of pancreatic cancer, reduce cancer cell

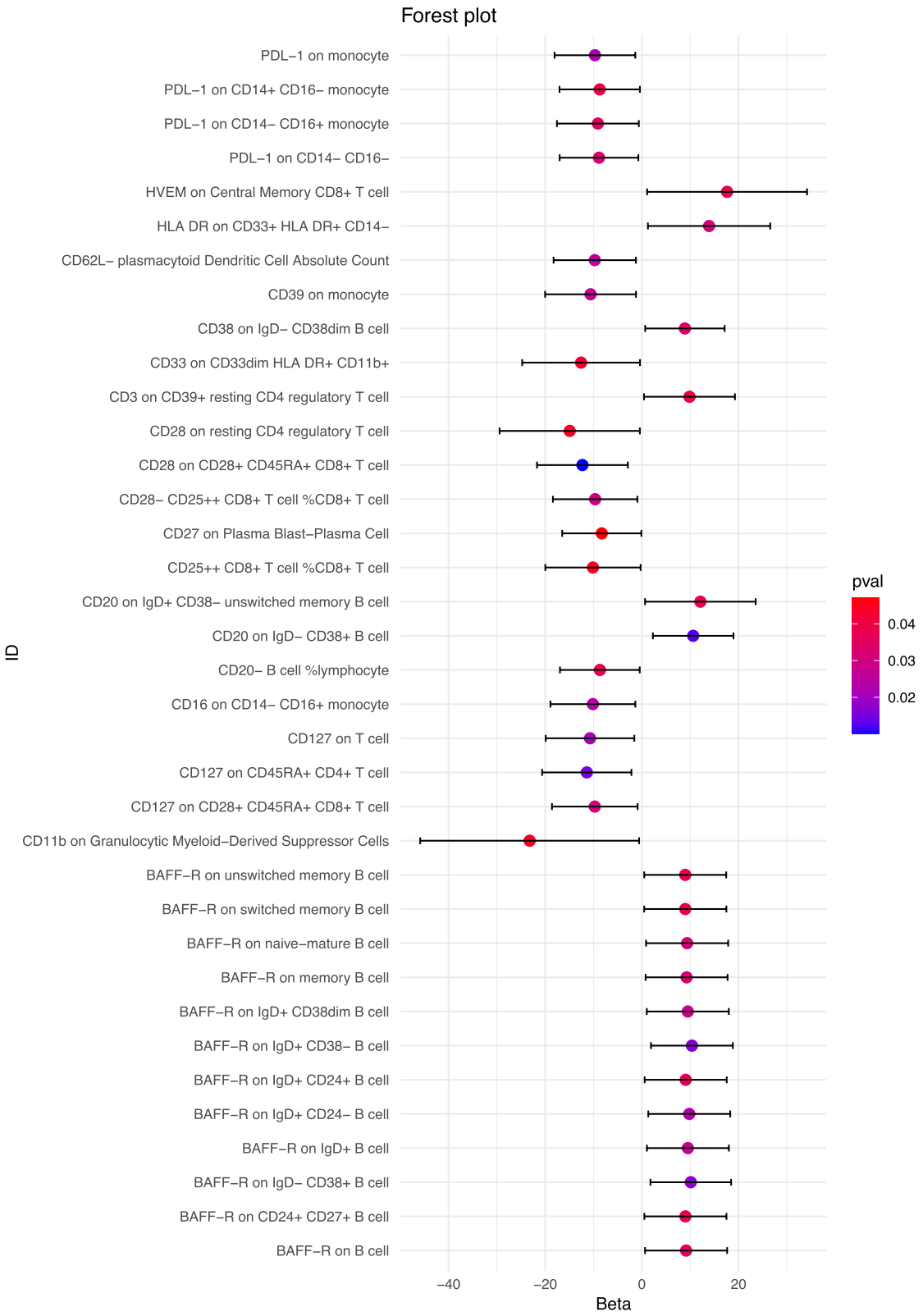

Fig. 3 Reverse MR analysis using the inverse variance weighting method

Table 4 Reverse MR sensitivity analysis

Panel	Trait	IVW		MR-Egger	
		Q	P	intercept	P
lymphocyte count	CD20- B cell %lymphocyte	5.628424468	0.583742028	−0.020197223	0.465393037
leukocyte count	CD62L-plasmacytoid Dendritic Cell Absolute Count	0.481777286	0.998053232	−0.009588601	0.734553115
lymphocyte count	CD28-CD25 + + CD8 + T cell %CD8 + T cell	8.111715967	0.322846124	0.036576174	0.207072277
lymphocyte count	CD25 + + CD8 + T cell %CD8 + T cell	8.86756079	0.262305067	−0.010806053	0.757103591
Blood protein measurement	BAFF-R on CD24 + CD27 + B cell	3.635212696	0.820703327	−0.007719359	0.781423826
Blood protein measurement	BAFF-R on IgD + CD24 + B cell	3.259441752	0.860009693	−0.010413602	0.708911623
blood protein measurement	BAFF-R on IgD + CD24- B cell	3.314789403	0.854435804	−0.003795162	0.891058846
blood protein measurement	BAFF-R on IgD + CD38- B cell	2.724797468	0.909240835	−0.008305874	0.764810477
blood protein measurement	BAFF-R on IgD + CD38dim B cell	3.487451321	0.836552833	−0.003621699	0.89607949
blood protein measurement	BAFF-R on IgD- CD38 + B cell	3.686630474	0.815080667	−0.003689713	0.892575379
blood protein measurement	BAFF-R on memory B cell	2.875102266	0.896310832	−0.006849821	0.805156326
blood protein measurement	BAFF-R on naive-mature B cell	3.239184768	0.862029417	−0.000763744	0.978039826
blood protein measurement	BAFF-R on unswitched memory B cell	3.645817664	0.819547994	−0.007521536	0.786646829
blood protein measurement	BAFF-R on switched memory B cell	3.7621677	0.806727296	−0.005189773	0.85188811
blood protein measurement	BAFF-R on IgD + B cell	3.063922391	0.879026562	−0.004646516	0.866957854
blood protein measurement	CD20 on IgD + CD38- unswitched memory B cell	2.464726428	0.929729695	0.020473805	0.587666815
blood protein measurement	CD20 on IgD- CD38 + B cell	0.925006408	0.995949307	−0.009793226	0.720995495
blood protein measurement	CD27 on Plasma Blast-Plasma Cell	3.339169887	0.851955298	0.001049838	0.968784009
blood protein measurement	CD38 on IgD- CD38dim B cell	4.616458973	0.706652061	0.009888258	0.714548601
blood protein measurement	BAFF-R on B cell	3.205047667	0.865407897	−0.002918699	0.916214953
blood protein measurement	CD3 on CD39 + resting CD4 regulatory T cell	4.568867206	0.712409418	−0.026788447	0.403698095
blood protein measurement	HVEM on Central Memory CD8 + T cell	10.62789262	0.155693853	−0.027090676	0.63858879
blood protein measurement	CD28 on CD28 + CD45RA + CD8 + T cell	5.107595069	0.64683467	−0.022517181	0.477739158
blood protein measurement	CD28 on resting CD4 regulatory T cell	1.05037159	0.591445467	−0.037334119	0.492576982
blood protein measurement	CD127 on T cell	7.08826735	0.419747781	−0.029800936	0.343497442
blood protein measurement	CD127 on CD28 + CD45RA + CD8 + T cell	1.235454188	0.990087531	−0.000590536	0.983931563
blood protein measurement	CD127 on CD45RA + CD4 + T cell	1.775880353	0.971198017	−0.022660552	0.468573891
blood protein measurement	CD33 on CD33dim HLA DR + CD11b +	4.626984466	0.70537716	0.032374968	0.432719247
blood protein measurement	CD16 on CD14- CD16 + monocyte	7.688509066	0.360860369	0.017070218	0.575814903
blood protein measurement	PDL-1 on CD14 + CD16- monocyte	4.837961663	0.679729842	0.002470782	0.9276554
blood protein measurement	PDL-1 on CD14- CD16 + monocyte	6.964173444	0.432619632	−0.004478464	0.880622351
blood protein measurement	PDL-1 on CD14- CD16-	4.544092419	0.715401504	0.011752961	0.662384596
blood protein measurement	PDL-1 on monocyte	3.584069031	0.826242434	0.003783025	0.889996723
blood protein measurement	CD39 on monocyte	2.664831048	0.914182429	−4.62E-05	0.998814508
blood protein measurement	CD11b on Granulocytic Myeloid-Derived Suppressor Cells	1.799015922	0.406769757	−0.074417086	0.408088882
blood protein measurement	HLA DR on CD33 + HLA DR + CD14-	7.279325969	0.400387478	−0.04225331	0.32980815

proliferation and invasion by increasing IFN-γ secretion and FasL expression level [33, 34]. IFN-γ has been demonstrated to have a therapeutic effect on human malignancies [35, 36]. Additionally, DN T cells have exhibited cytotoxicity against lung cancer-derived cells in vitro, indicating their potential as a rational alternative therapy [37]. Favorable outcomes have also been reported using DN T cells as an ex vivo therapy for leukemia [38]. Ponzeta et al. investigated the interaction between the TME and DN T cells, revealing that neutrophils can modulate the function of TCR-$\alpha\beta^+$ DN T cells, playing a crucial role in antitumor immunity [38].

Lymphocytes play a pivotal role in the development of cancer. The present study demonstrate a positive association between lymphocyte %leukocyte and an increased risk of CRC. Cong Ma et al. conducted a retrospective study on lung cancer by examining data of 430 lung cancer patients and 158 healthy controls, as well as analyzing

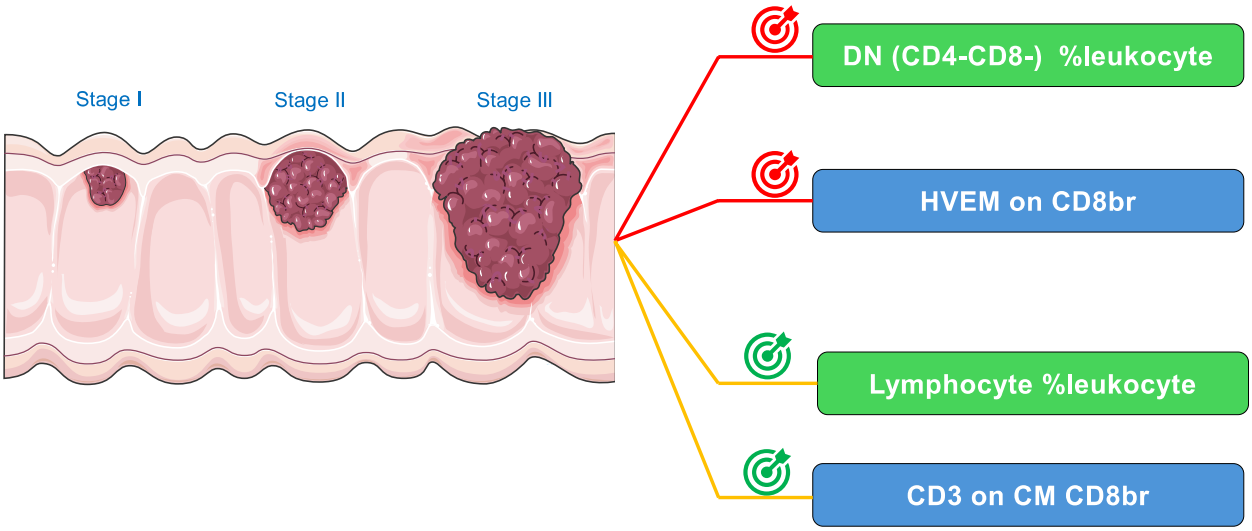

Fig. 4 Schematic summary of the study results. The red lines indicate immune cell phenotypes that are associated with a decreased incidence of CRC, while the yellow lines indicate those associated with an increased incidence. The green boxes represent the TBNK group, and the blue boxes represent the maturation stages in the T cell group

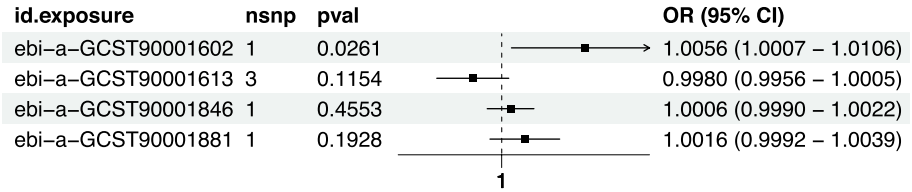

Fig. 5 Forest plot of MVMR analysis results. This forest plot displays the odds ratios (OR) and their 95% confidence intervals (CI) for four genetic variants analyzed in the MVMR study. The dashed line at OR = 1 indicates no association

20 clinical characteristics, including lymphocyte percentage. They found a strong correlation between a higher cancer risk and a lower lymphocyte percentage [39]. Jia Jun Ang et al. pointed out that the lymphocyte-to-white blood cell ratio (LWR) serves as a novel marker for postoperative morbidity in patients with CRC. In the multivariable analysis, only an LWR < 0.180 (odds ratio [OR]: 2.53, 95% confidence interval [CI]: 1.15–5.55) and neoadjuvant therapy (OR: 2.49, 95% CI: 1.16–5.24) were associated with overall morbidity [40]. However, findings of the present study contrast with those reported by Zhao et al. who found that patients with an increased LWR had significantly longer survival time compared with those with a decreased LWR in advanced cancer. They speculated that patients with an elevated LWR after palliative therapy may possess a stronger immune response, potentially improving patients' prognosis [41].

Early studies have demonstrated that central memory $CD8^+$ T cells (T_{CM}) could be considered more effective than effector memory T cells (T_{EM}) in mediating protective immunity [42]. In humans, T_{CM} cells exhibited a phenotypic profile of $CD45RA^-$ $CD45RO^+$ $CCR7^+$ $CD62L^+$, characterized by their lymph node homing properties [43, 44]. The presence of T_{CM} and T_{EM} cells has been found to be associated with a better prognosis in cancer patients. In fact, anti-CTLA-4 immunotherapy has exhibited to enhance the formation and maintenance of CD8 memory T cells in mouse infection models, potentially promoting memory against cancer [45]. Among patients with advanced melanoma treated with anti-CTLA4 immune checkpoint blockade (ICB) therapy, a higher proportion of $CD45RO^+$ memory cells within the total CD8 T cell population in the blood could serve as a positive indicator for predicting response rates and overall survival [46]. PD-1 expression level was higher in $T^{+++}{}_{EM}$ cells compared with that in T_{CM} cells [47]. In patients with advanced melanoma and non-small cell lung cancer, the frequency of $CD45RA^-$ $CCR7^+$ T^+CM

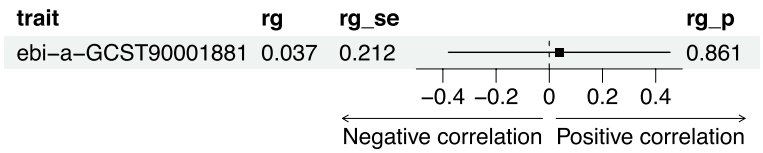

Fig. 6 Genetic correlation of HVEM on CD8bright T cells with CRC assessed using LDSC

cells in the blood has been shown to be a positive predictor of response and survival to anti-PD1 therapy [48, 49]. Responders with a higher TCM/TEFF ratio in the blood also exhibited a higher inflammatory gene expression profile in their tumors [48], indicating the importance of TCM cells in the antitumor immune response of patients. CD3 protein is a crucial molecule in the immune system, involved in activating cytotoxic T cells and T helper cells, being responsible for monitoring and defending against infections and abnormal cells in the body. CD3-bispecific antibodies (CD3-BsAbs) are an emerging therapeutic modality in cancer immunotherapy [50]. BsAbs can recognize different antigens with each antigen-binding domain, whereas traditional Abs recognize the same antigen through both Fab arms. CD3-BsAbs function by simultaneously binding to tumor-associated antigens expressed in tumor cells and CD3 in T cells [51].

HVEM serves as a molecular switch that activates stimulatory and inhibitory pathways that are crucial for T cell homeostasis. Upon binding to the canonical TNF-related molecule LIGHT, HVEM activates NF-kB, functioning as a costimulatory receptor during T cell activation [52]. The HVEM displays dual signaling in T cell activation, depending on its interacting ligands and intracellular effectors. An elevated HVEM expression level may exert immunosuppressive effects on some malignancies. Ma et al. [53] found that HVEM can serve as a favorable prognostic marker for intrahepatic cholangiocarcinoma (ICC), with costimulatory signals from HVEM potentially playing a dominant role in ICC progression. Additionally, HVEM functions as a ligand for BTLA, a member of the Ig superfamily that acts as an inhibitory signal receptor, limiting T cell function [54–56]. The BTLA/HVEM pathway plays a pivotal role in T cell suppression in tumors. Liu et al. [57] discovered that the BTLA/HVEM pathway may contribute to peripheral T cell suppression in patients with hepatocellular carcinoma.

The strength of the present study lies in the novel application of MR methods to investigate the relationship between immune cell phenotypes and the risk of CRC. The findings of the present study were derived under rigorous testing for horizontal pleiotropy, minimizing the confounding factors and the influence of reverse causality on the results. Furthermore, immune cell phenotypes that were significantly associated with the risk of CRC were identified, which have been less explored in previous studies.

However, the limitations of the present study should be pointed out. Firstly, a major constraint is the reliance on GWAS summary datasets for immune traits and CRC, which, although sourced from the reliable UK Biobank, might introduce potential biases due to differences in sample sizes, quality control methods, and other factors. Secondly, although sensitivity analysis alleviated concerns about pleiotropy, multivariate MR (MVMR) analysis would provide further insights into the relationship between immune phenotypes and the risk of CRC. Nevertheless, given the complexity of 731 exposures, including computational demands, statistical power, the validity of instrumental variables, and challenges in clinical interpretation, the application of MVMR is currently regarded infeasible. So this study conducts an application analysis of MVMR on immune cell phenotypes that have a causal relationship with the occurrence of colorectal cancer within the context of two-sample Mendelian randomization. Thirdly, the primarily European ancestry of the dataset, its limitation to adults, and the absence of stratification by gender and age may impact the generalizability and precision of the results. Furthermore, while Bonferroni correction was applied for multiple testing, the selection of IVs for immune cell phenotypes ($P < 1 \times 10^{-5}$) and the interpretation of results ($P_{Bonferroni} < 0.2$) were less stringent, potentially leading to some false positives due to the limited sample size.

Conclusions

Elevated levels of DN ($CD4^{-}CD8^{-}$) %leukocyte and HVEM on CD8br could serve as protective factors against CRC. Conversely, lymphocyte %leukocyte and CD3 on CM CD8br were identified as risk factors for CRC. Furthermore, using reverse Mendelian randomization, the present study did not detect a causal effect of CRC on immune phenotypes.

In conclusion, this study explored and demonstrated the causal effect of immune phenotype on colorectal cancer progression through a comprehensive bidirectional MR analysis. This enhances the current understanding of the correlation between immune responses and CRC risk, providing valuable insights for researchers to explore the biological mechanisms of CRC. However, it is imperative to underscore the necessity of validating our findings through rigorous clinical studies and fundamental research prior to their clinical implementation.

Abbreviations

CRC	Colorectal cancer
MR	Mendelian randomization
TBNK	T-cell/B-cell/NK-cell
HVEM	Herpesvirus entry mediator
IBD	Inflammatory bowel disease
TME	Tumor microenvironment
IVs	Instrumental variables
IVW	Inverse variance weighting
SNPs	Single-nucleotide polymorphisms
Treg	Regulatory T cells
cDC	Conventional dendritic cell
LWR	Lymphocyte-to-white blood cell ratio
T_{EM}	Effector memory T cells
CD3-BsAbs	CD3-bispecific antibodies
ICC	Intrahepatic cholangiocarcinoma
MVMR	Multivariate MR
LDSC	Linkage disequilibrium score regression

Supplementary Information

The online version contains supplementary material available at https://doi.org/10.1186/s12885-025-13701-3.

Supplementary Material 1.
Supplementary Material 2.
Supplementary Material 3.
Supplementary Material 4.
Supplementary Material 5.
Supplementary Material 6.
Supplementary Material 7.
Supplementary Material 8.
Supplementary Material 9.

Acknowledgements
We sincerely thank all the members who participated in this study and thank the contributors to the GWAS dataset. Finally, we would like to thank Editorbar Language Editing for providing us with language polishing services

Authors' contributions
All authors contributed to the paper. Fei Gao: Conceptualization; methodology. Qiaoli Zhang: Data curation; formal analysis; Fei Teng: Writing-original draft. Liling Li: Methodology; Software. Honglin Jiang: Validation; visualization. Wenna Li: Supervision. Chenxi Hu: Visualization. Zhongwen Lu: Writing—reviewing and editing. Yvxiang Wan: Writing–review and editing. Jinchang Huang: Supervision; Verifying the cited references. All authors read and approved the final article. The work reported in the article has been performed by the authors.

Funding
This study was funded by the Natural Science Foundation of China (No. 82074545 and 82205292); Project of the China Association of Chinese Medicine (CACM-2022-QNRC2-B02); Project of Beijing University of Chinese Medicine (2022-JYB-JBZR-042).

Data availability
All GWAS data were available on GWAS Catalog (https://www.ebi.ac.uk/gwas/). Immunophenotypes: accession numbers from GCST90001391 to GCST90002121.

Declarations

Ethics approval and consent to participate
All GWAS studies included in this paper were ethically approved by their institutions.

Consent for publication
All authors approved the submitted version.

Competing interests
The authors declare no competing interests.

Received: 16 April 2024 Accepted: 10 February 2025
Published online: 25 February 2025

References

1. Sung H, Ferlay J, Siegel RL, et al. Global Cancer Statistics 2020: GLOBOCAN estimates of incidence and mortality worldwide for 36 cancers in 185 countries. CA Cancer J Clin. 2021;71(3):209–49.
2. Keum N, Giovannucci E. Global burden of colorectal cancer: emerging trends, risk factors and prevention strategies. Nat Rev Gastroenterol Hepatol. 2019;16(12):713–32.
3. Ma H, Qi X. Red Meat Consumption and cancer risk: a systematic analysis of global data. Foods. 2023;12(22):4164.
4. Petersen GM, Slack J, Nakamura Y. Screening guidelines and premorbid diagnosis of familial adenomatous polyposis using linkage. Gastroenterology. 1991;100(6):1658–64.
5. de Visser KE, Joyce JA. The evolving tumor microenvironment: from cancer initiation to metastatic outgrowth. Cancer Cell. 2023;41(3):374–403.
6. Eich C, Vogt JF, Längst V, Clausen BE, Hövelmeyer N. Isolation and high-dimensional flow cytometric analysis of tumor-infiltrating leukocytes in a mouse model of colorectal cancer. Front Immunol. 2024;15:1295863.
7. Wang H, Tian T, Zhang J. Tumor-Associated Macrophages (TAMs) in Colorectal Cancer (CRC): from mechanism to therapy and prognosis. Int J Mol Sci. 2021;22(16):8470.
8. Siegel RL, Fedewa SA, Anderson WF, et al. Colorectal cancer incidence patterns in the United States, 1974–2013. J Natl Cancer Inst. 2017;109(8):djw322. https://doi.org/10.1093/jnci/djw322.
9. Sanderson E, Glymour MM, Holmes MV, et al. Mendelian randomization. Nat Rev Methods Primers. 2022;2:6.
10. Orrù V, Steri M, Sidore C, et al. Complex genetic signatures in immune cells underlie autoimmunity and inform therapy [published correction appears in Nat Genet. 2020 Sep 18;:]. Nat Genet. 2020;52(10):1036–45.
11. Richmond RC, Davey SG. Mendelian randomization: concepts and scope. Cold Spring Harb Perspect Med. 2022;12(1):a040501.
12. Gu J, Yan GM, Kong XL, Zhang YY, Huang LH, Lu HM. Assessing the causal relationship between immune traits and systemic lupus erythematosus by bi-directional Mendelian randomization analysis. Mol Genet Genomics. 2023;298:1493–503.
13. Wang C, Zhu D, Zhang D, Zuo X, Yao L, Liu T, et al. Causal role of immune cells in schizophrenia: Mendelian randomization (MR) study. BMC Psychiatry. 2023;23(1):590.
14. Xu M, Li C, Xiang L, et al. Assessing the causal relationship between 731 immunophenotypes and the risk of lung cancer: a bidirectional Mendelian randomization study. BMC Cancer. 2024;24(1):270. Published 2024 Feb 26.
15. Cao RR, Yu XH, Xiong MF, Li XT, Deng FY, Lei SF. The immune factors have complex causal regulation effects on bone mineral density. Front Immunol. 2022;13:959417.

16. Pierce BL, Ahsan H, Vanderweele TJ. Power and instrument strength requirements for Mendelian randomization studies using multiple genetic variants. Int J Epidemiol. 2011;40(3):740–52.
17. Kamat MA, Blackshaw JA, Young R, et al. PhenoScanner V2: an expanded tool for searching human genotype-phenotype associations. Bioinformatics. 2019;35(22):4851–3.
18. Bull CJ, Bell JA, Murphy N, et al. Adiposity, metabolites, and colorectal cancer risk: Mendelian randomization study. BMC Med. 2020;18(1):396.
19. Li Y, Ye D, Zhou W, Liu B, Mao Y, Sun X. Alcohol consumption and colorectal cancer risk: a Mendelian randomization study. Front Genet. 2022;23(13):967229.
20. Sato Y, Tsujinaka S, Miura T, Kitamura Y, Suzuki H, Shibata C. Inflammatory bowel disease and colorectal cancer: epidemiology, etiology, surveillance, and management. Cancers (Basel). 2023;15(16):4154.
21. Hemani G, Zheng J, Elsworth B, et al. The MR-Base platform supports systematic causal inference across the human phenome. Elife. 2018;7:e34408.
22. Burgess S, Thompson SG. Interpreting findings from Mendelian randomization using the MR-Egger method [published correction appears in Eur J Epidemiol. 2017 Jun 29;:]. Eur J Epidemiol. 2017;32(5):377–89.
23. Wu F, Huang Y, Hu J, Shao Z. Mendelian randomization study of inflammatory bowel disease and bone mineral density. BMC Med. 2020;18(1):312.
24. Brion MJ, Shakhbazov K, Visscher PM. Calculating statistical power in Mendelian randomization studies. Int J Epidemiol. 2013;42(5):1497–501. https://doi.org/10.1093/ije/dyt179.
25. Li Q, Guan X, Wu P, et al. Early transmission dynamics in Wuhan, China, of novel coronavirus-infected pneumonia. N Engl J Med. 2020;382(13):1199–207.
26. Sanderson E. Multivariable Mendelian Randomization and Mediation. Cold Spring Harb Perspect Med. 2021;11(2):a038984.
27. Burgess S, Thompson SG. Multivariable Mendelian randomization: the use of pleiotropic genetic variants to estimate causal effects. Am J Epidemiol. 2015;181(4):251–60.
28. Bulik-Sullivan BK, Loh PR, Finucane HK, et al. LD Score regression distinguishes confounding from polygenicity in genome-wide association studies. Nat Genet. 2015;47(3):291–5.
29. Alnaggar M, Xu Y, Li J, et al. Allogenic Vγ9Vδ2 T cell as new potential immunotherapy drug for solid tumor: a case study for cholangiocarcinoma. J Immunother Cancer. 2019;7(1):36.
30. Chitadze G, Oberg HH, Wesch D, Kabelitz D. The ambiguous role of γδ T lymphocytes in antitumor immunity. Trends Immunol. 2017;38(9):668–78.
31. Caccamo N, Dieli F, Meraviglia S, Guggino G, Salerno A. Gammadelta T cell modulation in anticancer treatment. Curr Cancer Drug Targets. 2010;10(1):27–36.
32. Correia DV, Lopes A, Silva-Santos B. Tumor cell recognition by γδ T lymphocytes: T-cell receptor vs. NK-cell receptors. Oncoimmunology. 2013;2(1):e22892.
33. Lu Y, Hu P, Zhou H, et al. Double-negative T cells inhibit proliferation and invasion of human pancreatic cancer cells in co-culture [published correction appears in Anticancer Res. 2020 Oct;40(10):5949]. Anticancer Res. 2019;39(11):5911–8.
34. Merims S, Li X, Joe B, et al. Anti-leukemia effect of ex vivo expanded DNT cells from AML patients: a potential novel autologous T-cell adoptive immunotherapy. Leukemia. 2011;25(9):1415–22.
35. Garris CS, Arlauckas SP, Kohler RH, et al. Successful Anti-PD-1 cancer immunotherapy requires T cell-dendritic cell crosstalk involving the cytokines IFN-γ and IL-12. Immunity. 2022;55(9):1749.
36. Takeda K, Nakayama M, Hayakawa Y, et al. IFN-γ is required for cytotoxic T cell-dependent cancer genome immunoediting. Nat Commun. 2017;8:14607.
37. Fang L, Ly D, Wang SS, et al. Targeting late-stage non-small cell lung cancer with a combination of DNT cellular therapy and PD-1 checkpoint blockade. J Exp Clin Cancer Res. 2019;38(1):123.
38. Lee J, Minden MD, Chen WC, et al. Allogeneic human double negative T cells as a novel immunotherapy for acute myeloid leukemia and its underlying mechanisms. Clin Cancer Res. 2018;24(2):370–82.
39. Ma C, Wang X, Zhao R. Associations of lymphocyte percentage and red blood cell distribution width with risk of lung cancer. J Int Med Res. 2019;47(7):3099–108.
40. Ang JJ, Chia DKA, Chan DKH. Lymphocyte-white cell ratio is a novel marker of morbidity following colorectal cancer surgery. J Surg Res. 2021;259:71–8.
41. Zhao W, Wang P, Jia H, et al. Lymphocyte count or percentage: which can better predict the prognosis of advanced cancer patients following palliative care? BMC Cancer. 2017;17(1):514.
42. Ichii H, Sakamoto A, Kuroda Y, Tokuhisa T. Bcl6 acts as an amplifier for the generation and proliferative capacity of central memory CD8+ T cells. J Immunol. 2004;173(2):883–91.
43. Sallusto F, Lenig D, Förster R, Lipp M, Lanzavecchia A. Two subsets of memory T lymphocytes with distinct homing potentials and effector functions. Nature. 1999;401(6754):708–12.
44. Sallusto F, Geginat J, Lanzavecchia A. Central memory and effector memory T cell subsets: function, generation, and maintenance. Annu Rev Immunol. 2004;22:745–63.
45. Pedicord VA, Montalvo W, Leiner IM, Allison JP. Single dose of anti-CTLA-4 enhances CD8+ T-cell memory formation, function, and maintenance. Proc Natl Acad Sci U S A. 2011;108(1):266–71.
46. Tietze JK, Angelova D, Heppt MV, et al. The proportion of circulating CD45RO+CD8+ memory T cells is correlated with clinical response in melanoma patients treated with ipilimumab. Eur J Cancer. 2017;75:268–79.
47. Duraiswamy J, Ibegbu CC, Masopust D, et al. Phenotype, function, and gene expression profiles of programmed death-1(hi) CD8 T cells in healthy human adults. J Immunol. 2011;186(7):4200–12.
48. Manjarrez-Orduño N, Menard LC, Kansal S, et al. Circulating T cell subpopulations correlate with immune responses at the tumor site and clinical response to PD1 inhibition in non-small cell lung cancer. Front Immunol. 2018;9:1613.
49. Fairfax BP, Taylor CA, Watson RA, et al. Peripheral CD8+ T cell characteristics associated with durable responses to immune checkpoint blockade in patients with metastatic melanoma. Nat Med. 2020;26(2):193–9.
50. Middelburg J, Kemper K, Engelberts P, Labrijn AF, Schuurman J, van Hall T. Overcoming challenges for CD3-bispecific antibody therapy in solid tumors. Cancers (Basel). 2021;13(2):287.
51. Dahlén E, Veitonmäki N, Norlén P. Bispecific antibodies in cancer immunotherapy. Ther Adv Vaccines Immunother. 2018;6(1):3–17.
52. Ware CF. Network communications: lymphotoxins, LIGHT, and TNF. Annu Rev Immunol. 2005;23(1):787–819.
53. Ma B, Meng H, Tian Y, et al. High expression of HVEM is associated with improved prognosis in intrahepatic cholangiocarcinoma. Oncol Lett. 2021;21(1):69.
54. Murphy KM, Nelson CA, Sedý JR. Balancing co-stimulation and inhibition with BTLA and HVEM. Nat Rev Immunol. 2006;6(9):671–81.
55. Murphy TL, Murphy KM. Slow down and survive: enigmatic immunoregulation by BTLA and HVEM. Annu Rev Immunol. 2010;28:389–411.
56. Sedý JR, Spear PG, Ware CF. Cross-regulation between herpesviruses and the TNF superfamily members. Nat Rev Immunol. 2008;8(11):861–73.
57. Liu J, Li J, He M, Zhang GL, Zhao Q. Distinct changes of BTLA and HVEM expressions in circulating CD4+ and CD8+ T cells in hepatocellular carcinoma patients. J Immunol Res. 2018;2018:4561571.

Publisher's Note